Carbohydrate Polymers 90 (2012) 399–406

Contents lists available at SciVerse ScienceDirect

Carbohydrate Polymers

journal homepage: www.elsevier.com/locate/carbpol

Biocomposite fiber of calcium alginate/multi-walled carbon nanotubes with enhanced adsorption properties for ionic dyes

Kunyan Sui*, Yujin Li, Rongzhan Liu, Yang Zhang, Xin Zhao, Hongchao Liang, Yanzhi Xia*

State Key Laboratory Cultivating Base for New Fiber Materials and Modern Textiles, Department of Polymer Science and Engineering, Qingdao University, Qingdao 266071, PR China

ARTICLE INFO

Article history:
Received 27 February 2012
Received in revised form 13 May 2012
Accepted 19 May 2012
Available online 27 May 2012

Keywords:
Calcium alginate
Multi-walled carbon nanotubes
Biocomposite fibers
Methylene blue
Methyl orange
Adsorption

ABSTRACT

A bioadsorbent of calcium alginate/multi-walled carbon nanotubes (CA/MWCNTs) composite fiber was fabricated by wet spinning and was characterized. Adsorptions of methylene blue (MB) and methyl orange (MO) ionic dyes onto CA/MWCNT composite fibers were investigated with different MWCNTs content and pH values. The results showed that introduction of MWCNTs of CA/MWCNTs composite fiber could not only sharply increase the adsorption capacity of MO onto bioadsorbent by 3 times, but enhanced the adsorption rate for MB compared to that of native CA fiber. Adsorption kinetics was determined by fitting pseudo-first, second-order and the intra-particle diffusion models to the experimental data, with the second-order model providing the best description of MB and MO adsorption onto CA/MWCNT fibers. The equilibrium adsorption data were analyzed by two widely applied isotherms: Langmuir and Freundlich. The desorption experiments showed the percentage of desorption were found to be 79.7% and 80.2% for MB and MO, respectively.

1. Introduction

The contamination of water from toxic compounds, like heavy metals and dyes remains a severe environmental and public problem. The treatment of industrial waste water is a challenging topic in environmental science, as the control of water pollution has become of increasing importance in recent years (Crini, 2006). A number of promising techniques have been established for elimination of heavy metals and dyes from contaminated waters. Adsorption appears to offer the best advantages, although the chemical degradation and the biodegradation approaches also find applications (Fugetsu et al., 2004; Salleh, Mahmoud, Karim, & Idris, 2011).

Adsorption is a well-known equilibrium separation process, in which the adsorbent may be of mineral (Borghi, Fabbri, Fiorini, Mancini, & Ribani, 2011; Chen, Gunawan, & Xu, 2011; Cheng, Huang, & Lee, 2011), organic or biological origin (Bird, Brough, Dixon, & Batchelor, 2006; Crini, 2005; Demirbas, 2009; Fan, Luo, Lv, Lu, & Qiu, 2011; Kavianinia, Plieger, Kandile, & Harding, 2012; Smith, Fowler, Pullket, & Graham, 2009; Wan Ngah, Teong, & Hanafiah, 2011; Xie, Zhao, & He, 2011). Alginate, extracted mainly from brown seaweeds which is abundant in all the sea areas of the world (Donati & Paoletti, 2009; Gacesa, 1988), is one of the most effective biological adsorbents for several heavy metal ions (Abdel-Halim & Al-Deyab, 2011; Anna & Hoek, 2010; Bayramoglu & Yakup Arica, 2009; Bhattacharyya, Dutta, De, Ray, & Basu, 2010; Davis, Volesky, & Mucci, 2003; Gok & Aytas, 2009; Kalis, Davis, Town, & Van Leeuwen, 2009; Perullini, Jobbágy, Mouso, Forchiassin, & Bilmes, 2010). However, the adsorption capacities of alginate for some dyes are barely satisfactory.

Carbon nanotubes (CNTs) have large specific surface areas and have been found the utility as adsorbents for both aqueous organic and inorganic contaminants (Ai et al., 2011; Hyung & Kim, 2008; Madrakian, Afkhami, Ahmadi, & Bagheri, 2011; Mauter & Elimelech, 2008; Tóth et al., 2012; Yan, Chang, Zheng, & Ma, 2011; Yan et al., 2005; Yang, Jing, Wu, Zhu, & Xing, 2010; Zhang, Shao, & Karanfil, 2011). However, widespread usage of CNTs will cause increasing emissions to the water environment and result in human contact risk to CNTs (Ali-Boucetta et al., 2011; Magrez et al., 2006; Som, Wick, Krug, & Nowack, 2011). Another adverse factor currently restricting the application of CNTs to environmental protection/remediation is their high costs.

These difficulties encountered in environmental applications with alginate and CNTs can be overcome by formation of calcium alginate/multi-walled carbon nanotubes (CA/MWCNTs) composite fiber. As defined in our laboratory, CA/MWCNT composite fiber was prepared using $CaCl_2$ as cross-linking agent by wet spinning. The composite fiber not only make full use of the heavy metals and dyes adsorption properties of alginate and MWCNTs, but also prevent MWCNTs from breaking off the composites to cause second micro-pollution to water. Such technique is also a practical approach to

* Corresponding authors. Tel.: +86 532 85950961; fax: +86 532 85950961.
E-mail address: kunyansui@163.com (K. Sui).

0144-8617/$ – see front matter © 2012 Elsevier Ltd. All rights reserved.
http://dx.doi.org/10.1016/j.carbpol.2012.05.057

overcome the high cost difficulty encountered in the use of CNTs for environmental remediation. Here, the adsorption properties for methylene blue (MB) and methyl orange (MO) organic dyes on CA/MWCNT composite fiber were characterized by using batch adsorption method.

2. Materials and methods

2.1. Materials

Sodium alginate (SA) was purchased from the Qingdao Mingyue Company (Qingdao, China) and it was used without further purification. Multi-walled carbon nanotubes (MWCNTs), purchased from Shenzhen Bill Science and Technology Corporation (Shenzhen, China), were produced by chemical vapor deposition. According to the manufacturer's specifications, the average diameter and length of MWCNTs were 30 nm and tens micrometer, respectively, with 95% purity. Methylene blue (MB) and methyl orange (MO) were purchased from Tianjin BASF Chemical Co. Ltd. (Tianjin, China). Calcium chloride ($CaCl_2$) was supplied by Shanghai Chemical Reagent.

2.2. Preparation of SA/MWCNT dispersions

Briefly, SA was dissolved in distilled water to produce a viscous solution with the concentration of 3 wt% SA after mechanical agitation for 4 h at ambient temperature and continue stirring for 30 min at 50 °C. Then different amount of MWCNTs were added into SA solution under constant stirring for 30 min at room temperature and then ultrasonic 15 min to achieve homogeneous dispersion.

2.3. Preparation of CA/MWCNT composite fibers

Spinning dope was prepared for different concentrations of nanotube and SA. A narrow jet of spinning solution was injected through a 0.5 mm diameter needle into a coagulation bath containing a 5 wt% aqueous solution of $CaCl_2$, and then collected on a spindle outside the bath which was rotated. The coagulation time was about 10 min. The coagulated fibers were then washed several times with deionized water and then dried in air under tension. The CA/MWCNT biocomposite fibers obtained had a linear-density of about 50 dtex.

2.4. Adsorption experiments

Adsorption experiments were performed in a 250 mL glass pyramid bottle. The expected pH was obtained by adjustment with 1 M HCl or 1 M NaOH solution using a pH meter (PHS-3G, pH meter precision). The suspensions containing different doses of fiber and the solutions of dyes were shaken with a magnetic stirrer. Samples were taken at different time intervals to carry out the kinetic study. All of the bottles were placed in a water bath at 25 ± 1 °C and shaken for 2 h. Throughout the experiment, the concentration of dyes before and after adsorption was measured by double-beam UV–vis spectrophotometer.

The adsorption amount q_t (mg/g) was calculated using the following equation:

$$q_t = \left(\frac{C_0 - C_t}{m}\right) V \quad (1)$$

where C_0 and C_t were the concentrations of dye in the solution before and after adsorption period of time (mg/L), respectively, m (g) was the mass of adsorbent and V (L) was volume of the dye solution.

The removed quantity of dye by the fibers was calculated as follows:

$$q_e = \left(\frac{C_0 - C_e}{m}\right) V \quad (2)$$

where C_0 (mg/L) represents the initial dye concentration, C_e (mg/L) is the equilibrium concentration of dye remaining in the solution, m (g) is the weight of dry fibers, and V (L) is the volume of the aqueous solution.

2.5. Characterization

The surface morphology and cross-sectional features of the fibers cutting by liquid nitrogen were characterized by scanning electron microscopy (SEM, JEOL JSM-6390LV). XRD patterns of the fibers were recorded on a Siemens D5005 X-ray powder diffractometer with Cu Ka (1.54051 A) radiation (40 kV, 40 mA). Samples were mounted on a sample holder and scanned with a step size of $2\theta = 0.01°$ between $2\theta = 3°$ and 50°.

3. Results and discussion

3.1. Characterization of CA/MWCNT composite fibers

Fig. 1 showed the SEM images of native CA and CA/MWCNT composite fibers. It can be observed that the fiber surface was rough and there are many channels on the surface of both native CA and CA/MWCNT composite fiber (Fig. 1a and b). From the large magnification of images, it can be seen that the cross section surface of CA fiber (Fig. 1c) was dense, as for CA/MWCNT composite fiber (Fig. 1d), there are many pore in the fiber and the implanted CNTs improve the surface area and pore volume of the alginate. MWCNTs were observed clearly in SEM images of the cross-section of the broken fibers, and the MWCNTs were dispersed well in the CA matrix. The diameter of the MWCNTs in the fibers was ca.50 nm, larger than that of the crude MWCNTs with 30 nm due to the surfaces of MWCNTs were wrapped by CA (Liu, Liang, Zhang, & Guo, 2006). The WAXD patterns of CA and CA/MWCNTs fibers were shown in Fig. 1e, respectively. For the pure CA fiber (Fig. 1e), the scattering peak at 13.5° (2θ) corresponds to the lateral packing among molecular chains, and the peak at 21.5° (2θ) is from the layer spacing along the molecular chain direction. Using the initial egg box model, we index the peak at 13.5° as (1 1 0) and the peak at 21.5 as (0 0 2) (Li, Fang, Vreeker, & Appelqvist, 2007). Compared to pure CA fiber, in addition to the diffraction peaks attributed to CA, the diffraction intensity of MWCNTs of the CA/MWCNTs composite fibers had also been observed. In Fig. 1e, a sharp reflection from the stacking of graphene layers in MWCNTs could be identified at ~26° (2θ) (Guo, Minus, Jagannathan, & Kumar, 2010). In hexagonal graphite, this reflection would be indexed as (0 0 2). The (0 0 2) reflection exhibited a high intensity along the equatorial direction, indicating that MWCNTs in the CA/MWCNTs composite fiber became oriented along the stretching direction. The results suggested that the oriented MWCNTs maybe act as micro-channels in matrix to improve the surface area of the CA/MWCNTs composites.

3.2. Effect of MWCNT dosage

The effects of MWCNTs content and contact time for the adsorption of MB onto CA/MWCNT fibers were studied for a period of 2 h for initial dye concentration of 100 mg/L, as depicted in Fig. 2a. It can be observed that the adsorption presented a two-stage kinetic behavior. For all the samples, with a rapid initial adsorption during the first 30 min, followed afterwards by a much slower rate, the adsorption was achieving a balance at 60 min. It can be explained that the initial fast adsorption for the first stage

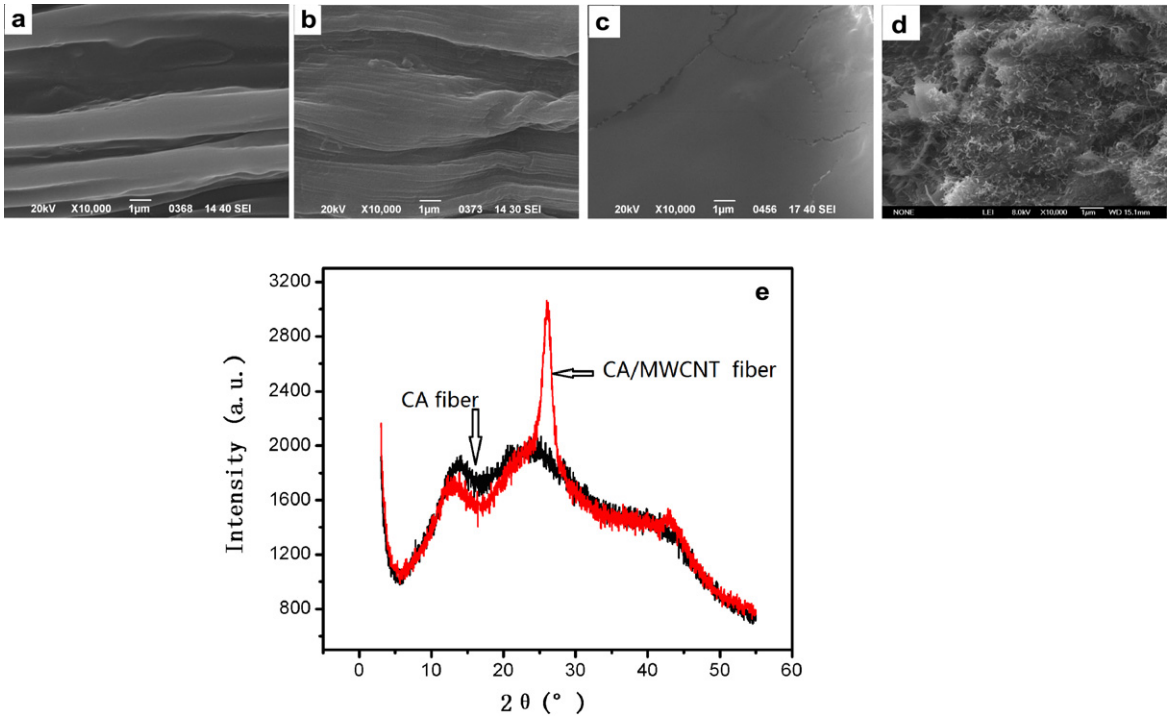

Fig. 1. Characterization of CA and CA/MWCNT fibers: (a–d) SEM images of CA and CA/MWCNT composite fibers; (e) WAXD curves of CA fiber and CA/MWCNTs fibers.

was physical interaction of a surface. Then the slow adsorption was MB in water to the fiber internal migration and proliferation, the processes were slow. From Fig. 2a, it can be observed that the amount of adsorption of MB for all the four adsorbents was nearly the same after 60 min adsorption reached equilibrium. It could indicate that SA played a major role on the adsorption capacity on MB for the CA/MWCNT composite fibers. Experimental results showed that the MB adsorption capacity (q_e) for CA and CA/MWCNT fibers was high to 181.5 and 182.5 mg/g, respectively. In addition, from the inset of Fig. 2a, it was noted that the adsorption rate of CA/MWCNT fibers for MB was increased with MWCNT content increasing at the initial adsorption stage. About 50.0% of dye was adsorbed on MB after 10 min for native CA and 5 min for CA/MWCNT fibers with the MWCNT content of 25.0%, respectively, suggesting that the oriented CNTs acting as micro-channels in composite fiber improve the surface area of the CA/MWCNTs adsorbent and enhance te adsorption rate of MB to the composite fibers.

As for the adsorption for MO, from Fig. 2b, it can be found that the adsorption capacity was improved to a great extent with the MWCNT content increasing for CA/MWCNT composite fibers. Results showed that the introduction of MWCNTs could increase the adsorption capacity of MO onto CA/MWCNT bioadsorbent with the MWCNT content increasing to about 25.0%, 3 times comparing with that of CA fiber. It was noted that the adsorption capacity of MO onto CA/MWCNTs composite fiber showed much higher than that of CA/MWCNTs hydrogel beads (Sui et al., 2010) due to the high surface area or pore volume of fiber (Supporting information). On the other hand, the low removal ability for CA fiber can be attributed to the fact that at pH 7.0, MO-type structure was with azo-negative charge, and the CA fiber surface may also be wrapped by negative charges due to the deprotonation

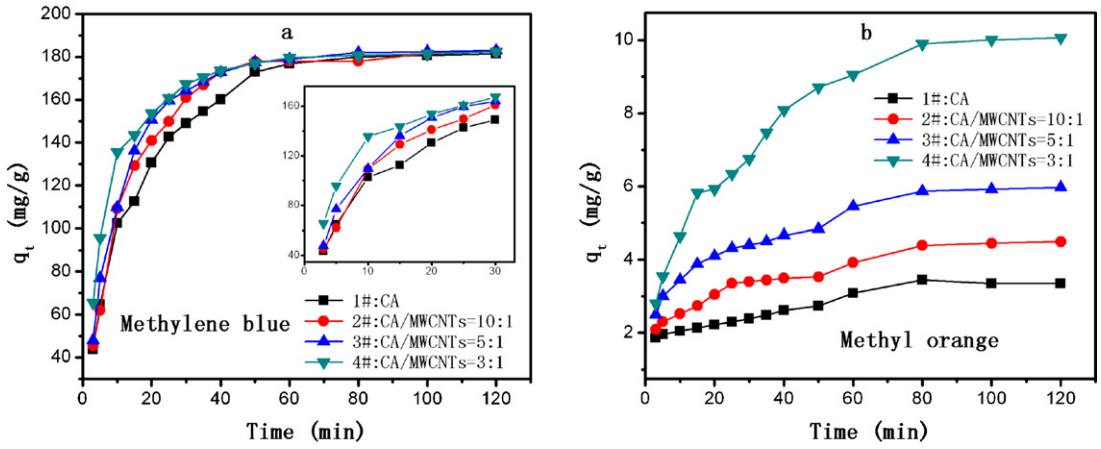

Fig. 2. Effect of MWCNTs content and contact time on the adsorption of (a) MB and (b) MO onto fibers (C_0 = 100 mg/L, pH 7.0).

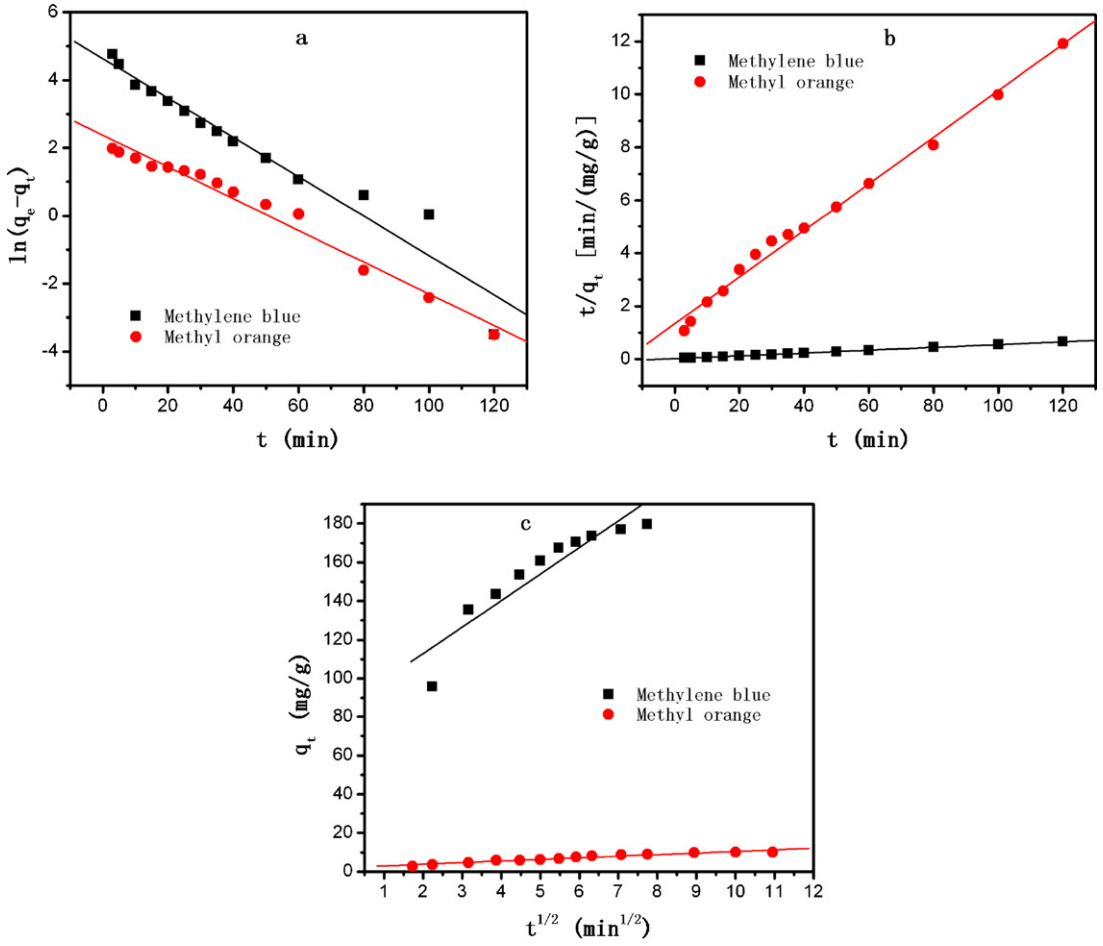

Fig. 3. Regressions of kinetic plots onto MB and MO: (a) pseudo-first-order model, (b) pseudo-second-order model and (c) intra-particle diffusion model (fiber 4#:CA/MWCNTs = 3:1).

of carboxyl group. Under such conditions, the MO cannot be adsorbed onto the surface of CA fibers because of the electrostatic repulsion.

Considering the above results, it could be concluded that the introduction of MWCNTs into CA fiber not only obviously increased the MO dye adsorption capability of CA, but also enhanced the adsorption rate for MB, which can be acted as a multi-purpose bio-adsorbent to not only cationic but anionic dyes with high adsorption efficiency.

3.3. Kinetic analyses

In order to elucidate the adsorption kinetics of cationic and anionic dyes on CA/MWCNTs fibers, three equations have been tested: pseudo-first order, pseudo-second order, intra-particle diffusion models. Fig. 3a–c displays the linear regressions.

The kinetic rate equations can be written as:

$$\frac{dq_t}{dt} = k_n(q_e - q_t)^n \tag{3}$$

where q_e and q_t correspond to the amount of dye adsorbed per unit mass of adsorbent (mg/g) at equilibrium and at time t, respectively, and k_n is the rate constant for nth order adsorption (k_n units are min^{-1} for $n = 1$ and $g\,mg^{-1}\,min^{-1}$ for $n = 2$). The linearized integrated forms of the equations are (Franca, Oliveira, & Ferreira, 2009):

The first order kinetic model is expressed as ($n = 1$):

$$\ln(q_e - q_t) = \ln q_e - k_1 t \tag{4}$$

where q_e and q_t are the amounts of adsorbate (mg/g) at equilibrium at time t (min), respectively, and k_1 is the rate constant of adsorption (min^{-1}). Values of k_1 were calculated from the plots of $\log(q_e - q_t)$ versus t. The experimental q_e values did not agree with the calculated, obtained from the linear plots (Table 1).

The second order kinetic model is expressed as ($n = 2$):

$$\frac{t}{q_t} = \frac{1}{k_2 q_e^2} + \frac{t}{q_e} \tag{5}$$

where k_2 ($g\,mg^{-1}\,min^{-1}$) is the rate constant of the second order adsorption. The parameters k_2 and q_e can be obtained from the

Table 1
Coefficients of pseudo-first and second-order adsorption kinetic models and intraparticle diffusion model.

Dye	Pseudo-first-order model			Pseudo-second-order model			Intraparticle diffusion model		
	k_1 (min^{-1})	$q_{e,cal}$ (mg/g)	R^2	k_2 (min^{-1})	$q_{e,cal}$ (mg/g)	R^2	k_i ($mg/g\,min^{1/2}$)	C (mg/g)	R^2
MB	0.05808	103.0	0.9432	0.00116	190.5	0.9997	13.688	85.534	0.8618
MO	0.04677	10.7	0.9777	0.00577	11.4	0.9918	0.825	2.193	0.9444

plot of (t/q_t) versus t, that should show a linear relationship. The calculated q_e values fit quite well with the experimental data and all of the correlation coefficients (R^2) are larger than 0.99 for both dyes (Table 1).

The effect of diffusion as the rate-controlling step in the adsorption was evaluated according to the intraparticle diffusion model (Kavitha & Namasivayam, 2007):

$$q_t = k_i t^{1/2} + c \quad (6)$$

where C is the intercept and k_i is the intraparticle diffusion rate constant (mg/g min$^{1/2}$), which can be evaluated from the slope of the linear plot of q_t versus $t^{1/2}$. The intra-particle diffusion model was utilized to determine the rate-limiting step of the adsorption process. If the regression of q_t versus $t^{1/2}$ is linear and passes through the origin, then intra-particle diffusion was the sole rate-limiting step (Yao, Xu, Chen, Xu, & Zhu, 2010). The regression is linear, but the plot does not pass through the origin (Fig. 3c), suggesting that the adsorption process is rather complex and involves more than one diffusive resistance. The values of the diffusion rate constant (C) and the regression coefficients (R^2) are given in Table 1.

Pseudo-first order, pseudo-second order and intraparticle diffusion kinetic models are illustrated in Fig. 3a–c and their coefficients are given in Table 1. As it can be seen, these adsorption systems follow a pseudo-second order kinetic model.

3.4. Effect of solution pH value

Initial pH value is one of the most important factors that affect the adsorption process. It affects not only the surface charge of the adsorbent, but also the ionization degree of the adsorbate. The experiments were carried out in pH range 2.0–12.0 and the results were illustrated in Fig. 4a and b. From Fig. 4a, it can be observed that, after the adsorption for 2 h, MB adsorption capacity increased sharply from 38.9 mg/g to 181.0 mg/g with pH increasing from 2.1 to 3.9, and then the content dyes adsorbed is not significantly changed with pH value above 4.0. Therefore, the optimum pH range for MB adsorption onto CA/MWCNTs bio-adsorbent was 4.0–12.0. The results showed that lower adsorption capacity was found in pH range 2.0–4.0, and it could be explained by the fact that more protons were available to protonate —COO^- groups to form —COOH group with positive charges because the SA has a pK_a value of 3.38 for mannuronic acid and 3.65 for guluronic acid (Chan & Neufeld, 2009), thereby enhancing the electrostatic repulsion between positively charged dye cations and positively charged surface of CA/MWCNTs. Above pH 4.0, a much larger amount of deprotonated COO^- negative groups was available for ionic interaction with cationic dye MB, leading to much larger amount of dye adsorbed on CA/MWCNTs.

As for MO adsorption, the data are presented in Fig. 4b. It was observed that dyes adsorbed decreased when pH increased from 2.0 to 12.0. As mentioned above, the contributions of MWCNTs adsorption played a major role on the adsorption capacity on MO for the CA/MWCNT composite fibers. It meant that the charge sign on the surface of MWCNT adsorbent should be negative in a wide pH range (i.e., 2.0–12.0). It was because that the surface of MWCNTs were wrapped by CA, with the pH increasing, the ionization of carboxyl groups on the surface can occur, leading to the surface of the CA/MWCNTs fibers being negatively charged. Excessive COO^- ions might compete with the dye anions and hence obvious reductions in dye uptake were observed. Therefore, the adsorption of MO by CA/MWCNTs fibers is favored at lower pH values.

3.5. Adsorption isotherms

The adsorption isotherms of MB and MO on CA/MWCNT fiber are shown in Fig. 5a–c. As can be seen from Fig. 5a, equilibrium uptake increased with the equilibrium dye concentrations increasing at the range of experimental concentration. This is a result of the increasing of the driving force from the concentration gradient. In the same conditions, if the concentration of dye in solution was higher, the active sites of CA/MWCNTs fibers were surrounded by much more dye ions, and the process of adsorption would carry out sufficiently. Therefore, the values of q_e increased with the equilibrium dye concentrations increasing.

The adsorption data were analyzed by the following two important isotherms: the Langmuir and Freundlich isotherms. The relationship between adsorption capacity of the fibers and dye concentration can be expressed using the Langmuir adsorption equation (Langmuir, 1918).

$$\frac{c_e}{q_e} = \frac{1}{q_m K_L} + \frac{1}{q_m} c_e \quad (7)$$

where C_e is the liquid-phase equilibrium concentration of dye (mg/g), q_e is the solid phase equilibrium concentration (mg/g), q_m is the maximum amount of dye per unit weight of adsorbent for complete monolayer coverage (mg/g), and K_L is the Langmuir adsorption equilibrium constant (L/mg), reflecting the energy of adsorption. When C_e/q_e was plotted against C_e, the straight line with slop $1/q_m$ was obtained (Fig. 5b), and the Langmuir constants K_L and q_0 were calculated from this isotherm and their values were listed in Table 2. From the correlation coefficients ($R^2 > 0.99$),

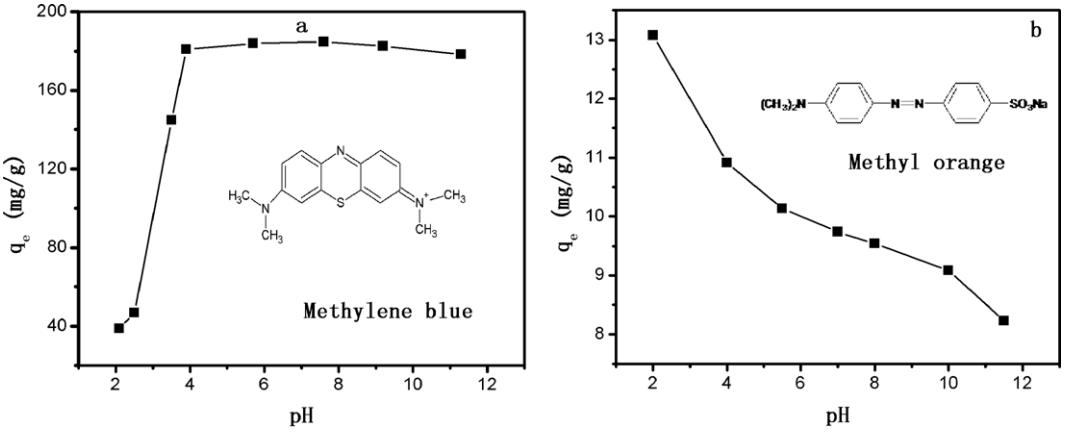

Fig. 4. Effect of pH value on the adsorption of (a) MB and (b) MO on fibers (fiber 4#:CA/MWCNTs = 3:1).

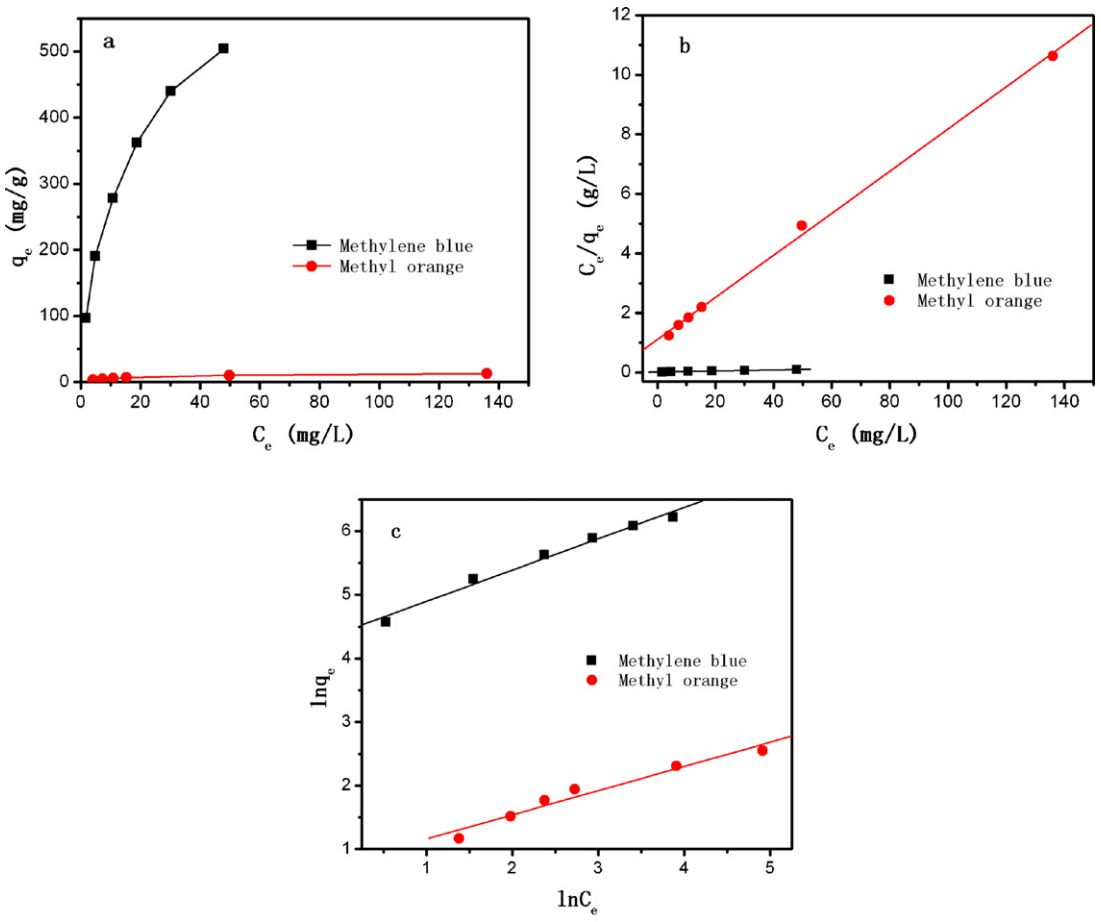

Fig. 5. Adsorption isotherms (a), Langmuir (b) and Freundlich (c) isotherms for MB and MO dye adsorption onto CA/MWCNTs fibers (fiber 4#:CA/MWCNTs = 3:1).

indicating that the adsorption of MB and MO on CA/MWCNT fiber follows the Langmuir isotherm. The maximum adsorption of MB and MO reached 606.1 and 12.5 mg/g. Comparing with other adsorbents, the CA/MWCNTs bio-composite fibers showed higher MB and MO adsorption capacities, for example, AC entrapped in magnetic alginate beads (AC-MAB) (Rocher, Siaugue, Cabuil, & Bee, 2008), Epichlorohydrin-reticulated magnetic alginate beads (EpiMAB) (Rocher, Bee, Siaugue, & Cabuil, 2010), and GG-MWCNT-Fe_3O_4 (Yan et al., 2011). It was found that the q_m values for the adsorption of MB and MO by AC-MAB (Rocher et al., 2008) were 22.060 and 0.655 mg/g, and by EpiMAB (Rocher et al., 2010) were 261.73 and 6.55 mg/g, and Yan et al. (2011) reported that the q_m value was 61.92 mg/g for the adsorption of MB by GG-MWCNT-Fe_3O_4. These comparisons suggested that CA/MWCNTs fiber had great potential as dye adsorbents in wastewater treatment.

Table 2
Langmuir and Freundlich isothermal adsorption equation parameters for the adsorption of MB and MO.

Isotherms	Parameters	Dye	
		MB	MO
Langmuir	q_m (mg/g)	606.1	12.5
	K_L (L/mg)	0.0916	0.0638
	R^2	0.9926	0.9980
	R_L	0.9909	0.9937
Freundlich	n	2.03	2.62
	K_F (mg/g (L/mg)$^{1/n}$)	81.84	2.17
	R^2	0.9845	0.9590

Furthermore, the essential characteristic of Langmuir equation can be expressed in terms of a dimensionless separation factor R_L (Sun, Zhang, Wu, & Liu, 2010), which is defined as

$$R_L = \frac{1}{1 + K_L C_0} \tag{8}$$

where K_L is the Langmuir constant and C_0 (mg/L) is the initial dye concentration. The value of R_L indicates the type of the isotherm to be either unfavorable ($R_L > 1$), linear ($R_L = 1$), favorable ($0 < R_L < 1$) or irreversible ($R_L = 0$). R_L values for MB and MO adsorption onto CA/MWCNTs fiber were less than 1 and greater than 0 indicating favorable adsorption (Table 2).

The Freundlich isotherm is an empirical equation employed to describe heterogeneous systems. The Freundlich equation (Luo & Zhang, 2009) is linearized as follows:

$$\ln\ q_e = \frac{1}{n} \ln c_e + \ln K_F \tag{9}$$

where q_e is the amount adsorbed at equilibrium (mg/g) and C_e is the equilibrium concentration of the dye (mg/L). K_F and n are Freundlich constants, K_F (mg/g (L/mg)$^{1/n}$) is the adsorption capacity of the adsorbent and n giving an indication of how favorable the adsorption process. It is generally stated that n values in the range 2–10 represent good, 1–2 moderately difficult, and less than 1 poor adsorption characteristics (Yao, He, Xu, & Chen, 2011). The plot of ln q_e versus ln C_e (Fig. 5c) gives straight lines with slop $1/n$. Fig. 5c shows that the adsorption of MB and MO also follows the Freundlich isotherm. Freundlich constants (K_F and n) were calculated and listed in Table 2. The studied materials are good adsorbents for MB ($n > 2$) and MO ($n > 2$).

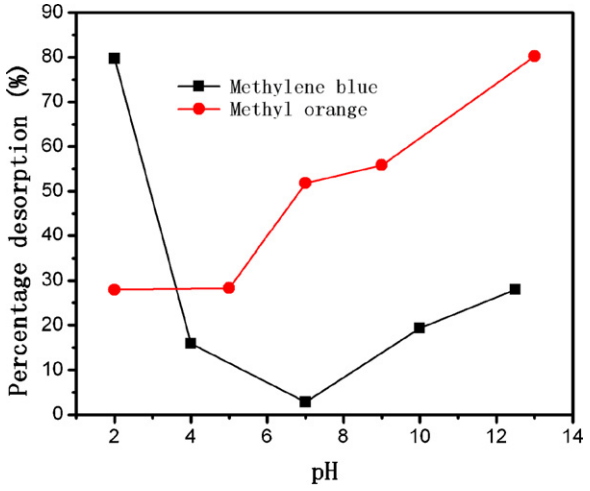

Fig. 6. Desorption of MB and MO of CA/MWCNTs composite fiber at different pH values (fiber 4#:CA/MWCNTs = 3:1).

3.6. Desorption

Desorption of the loaded dyes was carried out at pH 2.0–13.0 and the results are shown in Fig. 6. As can be seen from Fig. 6, the desorption capacity decreased for MB and increased for MO with pH values increasing. The results are corresponding to the adsorption experiments. In addition, the desorption efficiency were found to be 79.7% and 80.2% for MB at pH 2.0 and MO at pH 13.0, respectively.

4. Conclusions

A novel material, the CA/MWCNTs composite fiber as an effective bio-adsorbent for ionic dyes removal has been prepared. The adsorbent toward ionic dyes has higher adsorption capacity due to the introduction of MWCNTs and the large specific area of fiber form of the composite. Batch adsorption experiments showed that the adsorption process followed second-order kinetic model. The results suggested that the initial pH value is one of the most important factors that affect the adsorption capacity of the dyes onto CA/MWCNTs. The desorption experiments showed the percentage of the desorption were found to be 79.7% and 80.2% for MB at pH 2.0 and MO at pH 13.0, respectively, which were corresponding to the adsorption experiments. The CA/MWCNT composite fiber can be utilized as environment friendly bioadsorbent for the removal of ionic dyes from aqueous solution due to the efficient and fast adsorption process.

Acknowledgements

The authors appreciate the financial support to this research by the Natural Science Foundation of China (No. 50973047), program for Excellent Innovative Research Team of Shandong Province of China and Natural Science Foundation of Qingdao (No. 10-3-4-3-3-jch).

Appendix A. Supplementary data

Supplementary data associated with this article can be found, in the online version, at http://dx.doi.org/10.1016/j.carbpol.2012.05.057.

References

Abdel-Halim, E. S., & Al-Deyab, S. S. (2011). Removal of heavy metals from their aqueous solutions through adsorption onto natural polymers. *Carbohydrate Polymers*, *84*, 454–458.
Ai, L. H., Zhang, C. Y., Liao, F., Wang, Y., Li, M., Meng, L. Y., et al. (2011). Removal of methylene blue from aqueous solution with magnetite loaded multi-wall carbon nanotube: Kinetic, isotherm and mechanism analysis. *Journal of Hazardous Materials*, *198*, 282–290.
Ali-Boucetta, H., Al-Jamal, K. T., Müller, K. H., Li, S., Porter, A. E., Eddaoudi, A., et al. (2011). Cellular uptake and cytotoxic impact of chemically functionalized and polymer-coated carbon nanotubes. *Small*, *7*, 3230–3238.
Anna, J., & Hoek, E. M. V. (2010). Removing cadmium ions from water via nanoparticle-enhanced ultrafiltration. *Environmental Science and Technology*, *44*, 2570–2576.
Bayramoglu, G., & Yakup Arica, M. (2009). Construction a hybrid biosorbent using *Scenedesmus quadricauda* and Ca-alginate for biosorption of Cu(II), Zn(II) and Ni(II): Kinetics and equilibrium studies. *Bioresource Technology*, *100*, 186–193.
Bhattacharyya, A., Dutta, S., De, P., Ray, P., & Basu, S. (2010). Removal of mercury (II) from aqueous solution using papain immobilized on alginate bead: Optimization of immobilization condition and modeling of removal study. *Bioresource Technology*, *101*, 9421–9428.
Bird, J., Brough, N., Dixon, S., & Batchelor, S. N. (2006). Understanding adsorption phenomena: Investigation of the dye–cellulose interaction. *Journal of Physical Chemistry B*, *110*, 19557–19561.
Borghi, C. C., Fabbri, M., Fiorini, M., Mancini, M., & Ribani, P. L. (2011). Magnetic removal of surfactants from wastewater using micrometric iron oxide powders. *Separation and Purification Technology*, *83*, 180–188.
Chan, A. W., & Neufeld, R. J. (2009). Modeling the controllable pH-responsive swelling and pore size of networked alginate based biomaterials. *Biomaterials*, *30*, 6119–6129.
Chen, C., Gunawan, P., & Xu, R. (2011). Self-assembled Fe_3O_4-layered double hydroxide colloidal nanohybrids with excellent performance for treatment of organic dyes in water. *Journal of Materials Chemistry*, *21*, 1218–1225.
Cheng, H. P., Huang, Y. H., & Lee, C. (2011). Decolorization of reactive dye using a photo-ferrioxalate system with brick grain-supported iron oxide. *Journal of Hazardous Materials*, *188*, 357–362.
Crini, G. (2005). Recent developments in polysaccharide-based materials used as adsorbents in wastewater treatment. *Progress in Polymer Science (Oxford)*, *30*, 38–70.
Crini, G. (2006). Non-conventional low-cost adsorbents for dye removal: A review. *Bioresource Technology*, *97*, 1061–1085.
Davis, T. A., Volesky, B., & Mucci, A. (2003). A review of the biochemistry of heavy metal biosorption by brown algae. *Water Research*, *37*, 4311–4330.
Demirbas, A. (2009). Agricultural based activated carbons for the removal of dyes from aqueous solutions: A review. *Journal of Hazardous Materials*, *167*, 1–9.
Donati, I., & Paoletti, S. (2009). In B. H. A. Rehm (Ed.), *In alginate: biology and applications*. Berlin/Heidelberg: Springr-Verlarg.
Fan, L. L., Luo, C. N., Lv, Z., Lu, F. G., & Qiu, H. M. (2011). Removal of Ag^+ from water environment using a novel magnetic thiourea-chitosan imprinted Ag^+. *Journal of Hazardous Materials*, *194*, 193–201.
Franca, A. S., Oliveira, L. S., & Ferreira, M. E. (2009). Kinetics and equilibrium studies of methylene blue adsorption by spent coffee grounds. *Desalination*, *249*, 267–272.
Fugetsu, B., Satoh, S., Shiba, T., Mizutani, T., Lin, Y., Terui, N., et al. (2004). Caged multiwalled carbon nanotubes as the adsorbents for affinity-based elimination of ionic dyes. *Environmental Science and Technology*, *38*, 6890–6896.
Gacesa, P. (1988). Alginates. *Carbohydrate Polymers*, *8*, 161–182.
Gok, C., & Aytas, S. (2009). Biosorption of uranium(VI) from aqueous solution using calcium alginate beads. *Journal of Hazardous Materials*, *168*, 369–375.
Guo, H. N., Minus, M. L., Jagannathan, S., & Kumar, S. (2010). Polyacrylonitrile/Carbon Nanotube Composite Films. *Materials & Interfaces*, *5*, 1331–1342.
Hyung, H., & Kim, J. (2008). Natural organic matter (NOM) adsorption to multi-walled carbon nanotubes: Effect of NOM characteristics and water quality parameters. *Environmental Science and Technology*, *42*, 4416–4421.
Kalis, E. J. J., Davis, T. A., Town, R. M., & Van Leeuwen, H. P. (2009). Impact of ionic strength on Cd(II) partitioning between alginate gel and aqueous media. *Environmental Science and Technology*, *43*, 1091–1096.
Kavianinia, I., Plieger, P. G., Kandile, N. G., & Harding, D. R. K. (2012). New hydrogels based on symmetrical aromatic anhydrides: Synthesis, characterization and metal ion adsorption evaluation. *Carbohydrate Polymers*, *87*, 881–893.
Kavitha, D., & Namasivayam, C. (2007). Experimental and kinetic studies on methylene blue adsorption by coir pith carbon. *Bioresource Technology*, *98*, 14–21.
Langmuir, I. (1918). The adsorption of gases on plane surfaces of glass, mica and platinum. *Journal of the American Chemical Society*, *40*, 1361–1403.
Li, L. B., Fang, Y. P., Vreeker, R., & Appelqvist, I. (2007). Reexamining the Egg-Box Model in Calcium-Alginate Gels with X-ray Diffraction. *Biomacromolecules*, *8*, 464–468.
Liu, Y., Liang, P., Zhang, H. Y., & Guo, D. S. (2006). Cation-controlled aqueous dispersions of alginic-acid-wrapped multi-walled carbon nanotubes. *Small*, *2*, 874–878.
Luo, X. G., & Zhang, L. N. (2009). High effective adsorption of organic dyes on magnetic cellulose beads entrapping activated carbon. *Journal of Hazardous Materials*, *171*, 340–347.
Madrakian, T., Afkhami, A., Ahmadi, M., & Bagheri, H. (2011). Removal of some cationic dyes from aqueous solutions using magnetic-modified multi-walled carbon nanotubes. *Journal of Hazardous Materials*, *196*, 109–114.

Magrez, A., Kasas, S., Salicio, V., Pasquier, N., Seo, J. W., Celio, M., et al. (2006). Cellular toxicity of carbon-based nanomaterials. *Nano Letters*, *6*, 1121–1125.
Mauter, M. S., & Elimelech, M. (2008). Environmental applications of carbon-based nanomaterials. *Environmental Science and Technology*, *42*, 5843–5859.
Perullini, M., Jobbágy, M., Mouso, N., Forchiassin, F., & Bilmes, S. A. (2010). Silica-alginate-fungi biocomposites for remediation of polluted water. *Journal of Materials Chemistry*, *20*, 6479–6483.
Rocher, V., Bee, A., Siaugue, J., & Cabuil, V. (2010). Dye removal from aqueous solution by magnetic alginate beads crosslinked with epichlorohydrin. *Journal of Hazardous Materials*, *178*, 434–439.
Rocher, V., Siaugue, J., Cabuil, V., & Bee, A. (2008). Removal of organic dyes by magnetic alginate beads. *Water Research*, *42*, 1290–1298.
Salleh, M. A. M., Mahmoud, D. K., Karim, W. A. W. A., & Idris, A. (2011). Cationic and anionic dye adsorption by agricultural solid wastes: A comprehensive review. *Desalination*, *280*, 1–13.
Smith, K. M., Fowler, G. D., Pullket, S., & Graham, N. J. D. (2009). Sewage sludge-based adsorbents: A review of their production, properties and use in water treatment applications. *Water Research*, *43*, 2569–2594.
Som, C., Wick, P., Krug, H., & Nowack, B. (2011). Environmental and health effects of nanomaterials in nanotextiles and façade coatings. *Environment International*, *37*, 1131–1142.
Sui, K. Y., Xie, D., Gao, S., Wu, Z. M., Wu, W. W., & Xia, Y. Z. (2010). Preparation and adsorption properties of sodium alginate/multiwalled carbon nanotubes complex gel beads. *Gong Neng Cai Liao*, *41*, 268–270 (Chinese)
Sun, D. S., Zhang, X. D., Wu, Y. D., & Liu, X. (2010). Adsorption of anionic dyes from aqueous solution on fly ash. *Journal of Hazardous Materials*, *181*, 335–342.
Tóth, A., Voitko, K. V., Bakalinska, O., Prykhod'ko, G. P., Bertóti, I., Martínez-Alonso, A., et al. (2012). Morphology and adsorption properties of chemically modified MWCNT probed by nitrogen, n-propane and water vapor. *Carbon*, *50*, 577–585.
Wan Ngah, W. S., Teong, L. C., & Hanafiah, M. A. K. M. (2011). Adsorption of dyes and heavy metal ions by chitosan composites: A review. *Carbohydrate Polymers*, *83*, 1446–1456.
Xie, K. L., Zhao, W. G., & He, X. M. (2011). Adsorption properties of nano-cellulose hybrid containing polyhedral oligomeric silsesquioxane and removal of reactive dyes from aqueous solution. *Carbohydrate Polymers*, *83*, 1516–1520.
Yan, L., Chang, P. R., Zheng, P. W., & Ma, X. F. (2011). Characterization of magnetic guar gum-grafted carbon nanotubes and the adsorption of the dyes. *Carbohydrate Polymers*, *87*, 1919–1924.
Yan, Y. M., Zhang, M. N., Gong, K. P., Su, L., Guo, Z. Z., & Mao, L. Q. (2005). Adsorption of methylene blue dye onto carbon nanotubes: A route to an electrochemically functional nanostructure and its layer-by-layer assembled nanocomposite. *Chemistry of Materials*, *17*, 3457–3463.
Yang, K., Jing, Q. F., Wu, W. H., Zhu, L. Z., & Xing, B. S. (2010). Adsorption and conformation of a cationic surfactant on single-walled carbon nanotubes and their influence on naphthalene sorption. *Environmental Science and Technology*, *44*, 681–687.
Yao, Y. J., He, B., Xu, F. F., & Chen, X. F. (2011). Equilibrium and kinetic studies of methyl orange adsorption on multiwalled carbon nanotubes. *Chemical Engineering Journal*, *170*, 82–89.
Yao, Y. J., Xu, F. F., Chen, M., Xu, Z. X., & Zhu, Z. W. (2010). Adsorption behavior of methylene blue on carbon nanotubes. *Bioresource Technology*, *101*, 3040–3046.
Zhang, S. J., Shao, T., & Karanfil, T. (2011). The effects of dissolved natural organic matter on the adsorption of synthetic organic chemicals by activated carbons and carbon nanotubes. *Water Research*, *45*, 1378–1386.